



Research papers

Numerical simulation study of urban hydrological effects under low impact development with a physical experimental basis



Lidong Zhao, Ting Zhang*, Jianzhu Li, Libin Zhang, Ping Feng

State Key Laboratory of Hydraulic Engineering Simulation and Safety, Tianjin University, Tianjin 300072, China

ARTICLE INFO

This manuscript was handled by Corrado Corradini, Editor-in-Chief

Keywords:

Urban hydrological effects
Low impact development
Physical experiment
Numerical simulation

ABSTRACT

Global climate change and rapid urbanization led to frequent extreme rainstorms and waterlogging. Low impact development (LID) as an essential measure of urban stormwater control, it is necessary to explore the urban hydrological response under low impact development combined with physical experiment and numerical simulation. This paper takes the Beiyangyuan campus of Tianjin University, where numerous LID practices have been implemented, as the study area. The prototype permeable pavement in the campus was scaled down to a laboratory-scale for infiltration experiments. The results show that the Horton infiltration model could describe the infiltration process of permeable concrete and grass-planting brick. The initial infiltration rate of the permeable concrete is large but decays faster. In contrast, the infiltration process of the grass-planting brick decays slower, and the stable infiltration rate and infiltration capacity are higher than that of the permeable concrete. The mean infiltration rates measured for the permeable concrete and the grass-planting brick were 95 mm/hr and 190 mm/hr, respectively. A SWMM-MIKE21 coupled model was constructed based on the LID experimental results to explore the effects of the removal or density reduction of the LID practices on surface hydrological processes. The results show that permeable pavement performs best in the reduction of runoff volume, inundation area, and inundation depth, while the bio-retention cell takes the second place, and the sunken greenbelt has limited effect. Frequent light rainfall is sensitive to the density of LID practices, and the implementation of even a tiny percentage (4% of the catchment area) of LID practices can be effective in controlling runoff. The removal or density reduction of LID practices has little effect on the inundation region but leads to an increased possibility of flood risk due to increasing inundation depth.

1. Introduction

Global climate change is an indisputable fact, leading to frequent extreme precipitation events (IPCC, 2021). Accompanied by urban expansion which increases impermeable surfaces, the urban flooding disaster is becoming increasingly severe (Qiu 2012; Wu et al., 2020; Zhao et al., 2021). In order to improve the urban water cycle process, the concept of low impact development (LID) has been proposed (Fisher et al., 2007; Hamel et al., 2013; Shafique and Kim, 2015; Che et al., 2015). Related infrastructures such as bio-retention cell (BC), sunken greenbelt (SG) and permeable pavement (PP) are widely used in many countries.

China started the construction of Sponge Cities based on the core theory of low impact development in 2014, with significant resources invested in constructing pilot cities every year (Jia et al., 2017).

However, the mechanism of how LIDs control the urban stormwater yield and concentration process is still unclear, especially the study on the mechanism of LID practices in mitigating urban flood is still relatively weak. Whether LID practices are effective in solving urban flooding is still an issue being widely debated (Jia, 2017).

Physical experiment is a typical way of assessing LID performance (Sun et al., 2011; Kamali et al., 2017; Hou et al., 2019; Song et al., 2021). We can easily observe the changes in the local hydrological processes caused by LID practices through physical experiments. However, LID experiment is hard to represent the hydrological response of the whole city (Zhang et al., 2014a). In this situation, numerical modeling techniques can be applied to study the urban hydrological response under low impact development at multiple scales. Currently, urban hydrological models such as SWMM (Yin et al., 2021), MIKE Urban (Han et al., 2021), and L-THIA-LID (Li et al., 2019) are often used to study the effect

* Corresponding author.

E-mail addresses: zhaolidong@tju.edu.cn (L. Zhao), zhangting_hydro@tju.edu.cn (T. Zhang), lizhanzhu@tju.edu.cn (J. Li), 15098812157@163.com (L. Zhang), fengping@tju.edu.cn (P. Feng).

of LID practices on urban stormwater runoff reduction and their cost-effectiveness.

The accuracy of the LID parameters in the existing models is impossible to ensure in numerical simulation studies due to the lack of observational experiments on typical LID practices and sufficient measured data, and the reliability of simulation results has not yet been confirmed. (Ahiablame et al., 2012). In addition, the spatial heterogeneity of the study regions and LID practices (Dilley et al., 2005; Zhang et al., 2014b; Yang et al., 2022) also leads to a significant regional character of the research results. Therefore, obtaining valuable measured parameters from typical LID experiments and integrating them into numerical simulations of urban hydrological processes becomes an important research direction (Gilroy and McCuen, 2009; Lisenbee et al., 2022).

Current research on the hydrological response under low impact development based on numerical simulation mainly focuses on the low impact development reconstruction of conventional development regions (Liu et al., 2015; Son et al., 2017; Peng et al., 2020; Ye and Xu, 2022), and the optimization of the spatial distribution of LID practices based on single or multiple objectives (Ahiablame et al., 2012; Baek et al., 2015; Eckart et al., 2018; Xu et al., 2018), while the research on actual LID constructed cases is rarely reported. In order to further understand the effect of low impact development, it is necessary to systematically investigate the urban hydrological response in LID regions on a physical experimental basis.

In summary, studies on the urban hydrological response in LID regions combined with physical experiments and numerical simulations have not yet been thoroughly discussed. This work carried out experiments on the infiltration of typical permeable pavement with constant rainfall intensity based on an artificial rainfall experimental system, quantitatively analyzed its infiltration characteristics. A 1D-2D coupled urban hydrological numerical model of the study area with the experimental results was constructed to systematically quantify the effects of removing LID practices or reducing the density on the urban surface hydrological processes. The research objectives of this paper are: (1) to

quantitatively analyze the infiltration characteristics of typical LID practices based on physical experiments and to apply the measured infiltration parameters to subsequent numerical simulation studies; (2) to systematically investigate the surface hydrological response in LID regions based on the constructed SWMM-MIKE21 coupled model.

2. Materials and methods

2.1. Study area and data sets

This paper takes the Beiyangyuan Campus of Tianjin University as the study area, which is located in Jinnan District of Tianjin, China, with a latitude and longitude between $117^{\circ}17' - 117^{\circ}20'$ E and $38^{\circ}59' - 39^{\circ}01'$ N, covering an area of about 2.4 km^2 (Fig. 1). The Campus has a temperate, semi-humid continental monsoon climate with four distinct seasons, with summer concentrating about 70% of the annual rainfall. The study area is a coastal and river alluvial plain with low, flat topography, and the soil has high salinity and weak infiltration capacity.

Tianjin University is committed to making the Beiyangyuan campus a green ecological campus. It has implemented many LID practices on campus over the years, mainly including bio-retention cells, sunken greenbelt, and permeable pavement. Therefore, as an implemented pilot sponge campus, the study area is an exemplary case study for exploring the effect of LID practices on urban hydrological process.

In this paper, the primary data and materials for constructing the model were collected, mainly including topographical data of the study area, drainage system data, *Tianjin University Stormwater Utilization and Drainage Engineering Planning*, etc. The above data and materials were provided by the Department of Logistics and Infrastructure of Tianjin University. GF-2 data (<https://36.112.130.153:7777/DSSPlatform/productSearch.html> accessed on 31 October 2022) for the study area were collected to extract the land use type, which is shown in Fig. 1. Two observed rainfall events (9 October 2017 and 23 July 2018) and water depth data were collected for parameter calibration and model verification. The locations of the rainfall gauge and radar water level gauge in

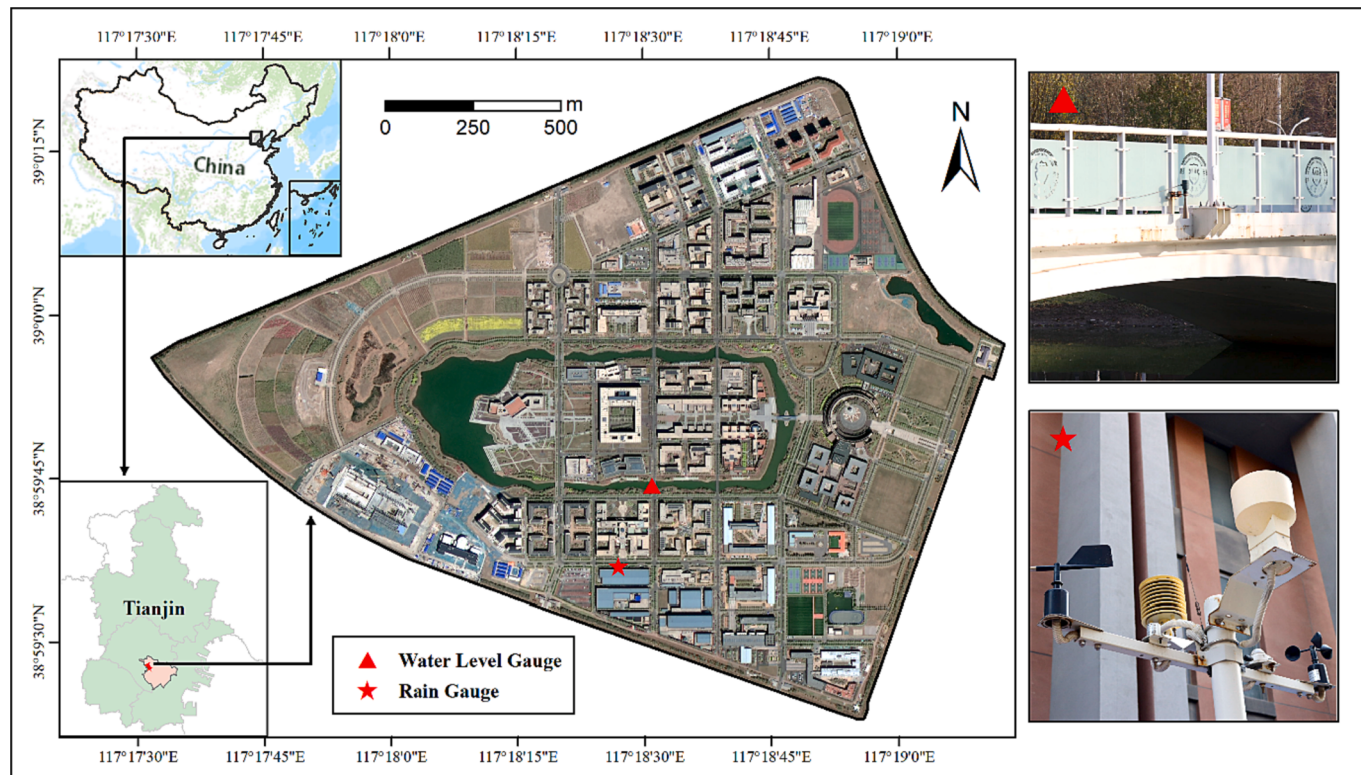


Fig. 1. Geographical location of the study area and location of the measured sites.

the study area are shown in Fig. 1.

2.2. Experimental design

According to the distribution of LID practices in the study area, the prototype permeable pavement structure within the campus was scaled down to a laboratory-scale. Based on the artificial rainfall experimental system (Fig. S1), a constant rainfall intensity infiltration experiment was designed to identify the infiltration characteristics of two typical permeable pavements quantitatively, including permeable concrete and grass-planting brick.

The experimental tank was constructed according to the collected design drawings (Fig. S2) and instructions in Tianjin University. The surface of the permeable concrete and grass-planting brick for experiment is shown in Fig. 2.

The experiment is based on the Artificial Rainfall Method (Miu, 2007) with a constant rainfall intensity of 10 mm/min. The same experimental initial conditions were controlled through the antecedent dry period in daytime (ADP daytime). The experiment was repeated 3 times to reduce the measure errors. When conducting artificial rainfall experiments, the outflow process was continuously recorded, rainfall can be stopped once the outflow is stabilized. Ignoring evaporation during the rainfall period, the infiltration rate can be expressed by the water balance equation as follows:

$$f(t) = i(t) - r(t) \quad (1)$$

where $f(t)$ is the infiltration rate at time t , mm/min; $i(t)$ is the rainfall intensity at time t , mm/min; and $r(t)$ is the runoff intensity at time t , mm/min.

2.3. Design rainstorm

LID practices are spatially classified as green infrastructure in sponge city construction, also known as “small sponges”, and are used for source control, mainly for frequent light rainfall events (Huang, 2018). Therefore, the design rainstorm return period should not be too large. In this paper, 1, 2, 3 and 4-year return period were selected as the design rainstorm with a rainfall duration of 2 hrs.

Due to the lack of observed long-term rainfall data series, the design rainstorm was calculated based on the equations in *Tianjin Sponge City Construction Technical Guidelines* (2016). In the Guidelines, the entire Tianjin city is divided into four rainstorm zones according to the characteristics of rainstorms (Fig. S3), and the study area is located in Zone I. According to the Guidelines, the 1-year return period rainstorm intensity of Zone I is given in Table S1, and the calculation formula for the 2-year to 100-year return period rainstorm intensity is as follows:

$$q = \frac{2141(1 + 0.7562\lg T)}{(t + 9.6093)^{0.6893}} \quad (2)$$

where q is the design rainstorm intensity, $L \cdot (s \cdot hm^2)^{-1}$; t is the rainfall duration, min. T is the design return period, a.

According to the rainfall intensity under 1-year return period (Table S1) and formula (2), the 2 hr rainfall intensity and total rainfall under different return periods were calculated as shown in Table 1. As the 1-year return period in the *Tianjin Sponge City Construction Technical Guidelines* only gives the total rainfall volume but not the rain pattern, the 1-year return period rainfall time distribution in this study is obtained by using the time distribution pattern of the 2 to 100-year return period (Table S2). According to Table 1 and Table S2, the rainfall process of the 2hr design rainstorm under different return periods is calculated, shown in Fig. 3.

2.4. Modeling implementation

Currently, existing urban rainfall-runoff models such as SWMM (Rui et al., 2015) and ILLU-DAS (Tsihrintzis and Sidan, 2008) can meet the needs of urban storm drainage system simulation, but cannot simulate surface hydrological processes. Some researchers have coupled SWMM with other 2D surface flow models to simulate surface hydrological processes, such as SWMM and Iber coupling (Sañudo et al., 2020), SWMM and MIKE21 coupling (Yang et al., 2020; Zhao et al., 2021). Based on these previous studies, the SWMM and MIKE21 coupled models was established to simulate the hydrological process under LID in this study. Readers are referred to Rossman (2015), DHI (2022) and Zhao et al. (2021) for more details on the SWMM and MIKE21 models and their coupled approach.

The reasonable use of remote sensing data to extract information such as buildings helps the division of subcatchments (Zhang et al., 2018). In this paper, the land use types, including LID practices in the study area, were obtained from the GF-2 data, combined with field investigations and the *Green Campus Construction Plan of Tianjin University* (Fig. 4a). Based on the topographic slope, drainage network system, drainage zoning, and land use type, the study area was divided into 59 subcatchments with 124 Junctions, 15 outfalls, 2 pumps, and 123 conduits. The digital elevation model was modified based on the measured building step heights from the field investigation to avoid overestimation of the ponding depth (Zhao et al., 2021), and the final SWMM and MIKE21 coupled model generalization is shown in Fig. 4b.

In order to evaluate the reliability of the model, the determination coefficient (R^2), the Nash-Sutcliffe efficiency (NSE), and the root mean square error (RMSE) were used to quantitatively evaluate the degree of

Table 1
Design rainfall intensity under different return periods (2hr).

Return Period (yr)	1	2	3	4
Rainfall Intensity ($L \cdot (s \cdot hm^2)^{-1}$)	39.245	91.928	101.899	108.974
Total rainfall (mm)	28.3	66.2	73.4	78.5



Fig. 2. The permeable pavement underlying surface of the experimental tank.

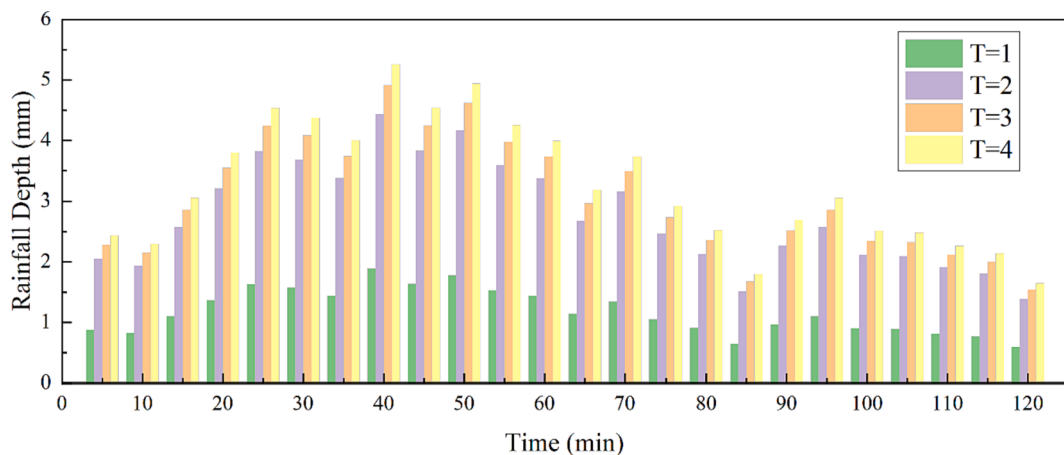


Fig. 3. Design rainstorm processes under different return periods.

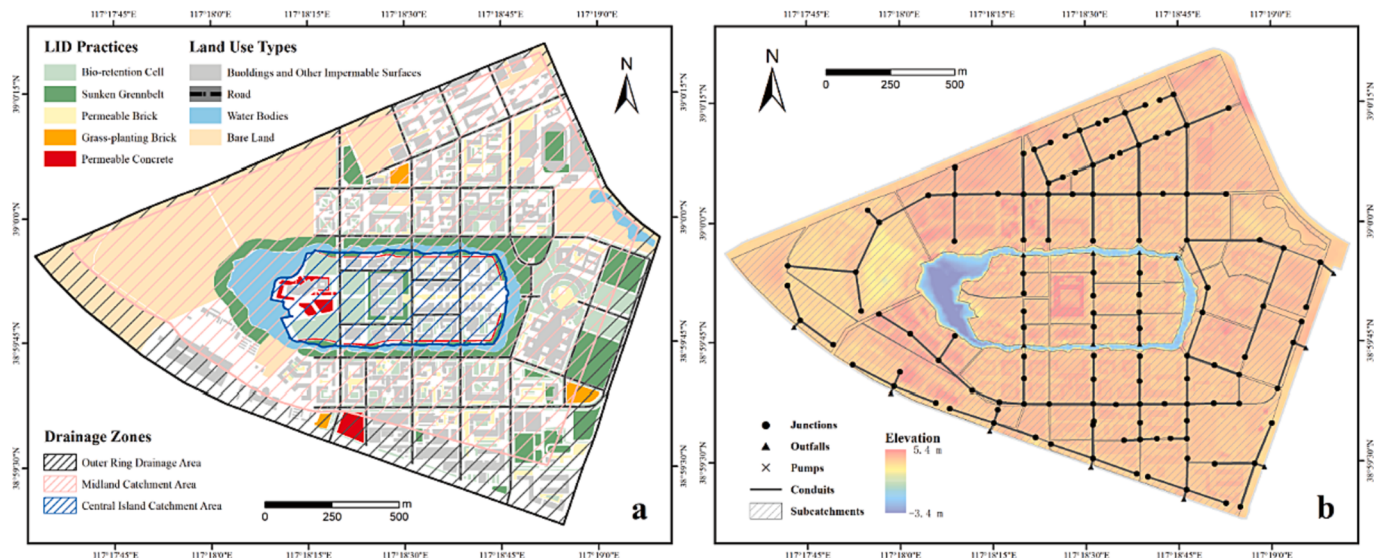


Fig. 4. (a) Land use types and drainage zoning; (b) results of the coupled model generalization.

agreement between the simulated and observed water depths in the river. The calculation formulas are as follows:

$$R^2 = \frac{\sum_{i=1}^n (H_{o,i} - \bar{H}_o)(H_{s,i} - \bar{H}_s)}{\sum_{i=1}^n (H_{o,i} - \bar{H}_o)^2 \sum_{i=1}^n (H_{s,i} - \bar{H}_s)^2} \quad (3)$$

$$NSE = 1 - \frac{\sum_{i=1}^n (H_{o,i} - H_{s,i})^2}{\sum_{i=1}^n (H_{o,i} - \bar{H}_o)^2} \quad (4)$$

$$RMSE = \sqrt{\frac{1}{n} \sum_{i=1}^n (H_{s,i} - H_{o,i})^2} \quad (5)$$

where, $H_{o,i}$ and $H_{s,i}$ are the observed and simulated water depth at time i , m; \bar{H}_o and \bar{H}_s are the mean of the observed and simulated water depth, respectively, m.

2.5. Scenario design

Based on the implemented LID practices in the study area, LID removal and density reduction scenarios were set up to quantitatively analyze their impact on the surface hydrological processes. Taking 100% of the existing LID practices in the study area as a reference, three LID

removal scenarios (Fig. 5) were set: (1) the removal of bio-retention cells, noted as BC-0%; (2) the removal of permeable pavements (including permeable brick, grass-planting brick, and permeable concrete), noted as PP-0%; (3) the removal of sunken greenbelt, noted as SG-0%. Based on the existing LID practices, 20% area in proportion to each LID practice was reduced successively to obtain six LID density reduction scenarios (Fig. 6).

The removal or density reduction of LID practices does not change the subcatchment to which the LID practices belong. Considering the actual situation of the LID practices implementation, the replacement of the area occupied by the original LID practices after the LID removal or density reduction is described as follows: permeable pavement is replaced with impermeable surface; sunken greenbelt and bio-retention cell are replaced with permeable surface. After LID removal or density reduction, relevant parameters need to be changed, including the impermeability of the subcatchments, the area of each LID practice, the proportion of impervious area treated, the proportion of pervious area treated, and the surface width per unit (permeable pavement only).

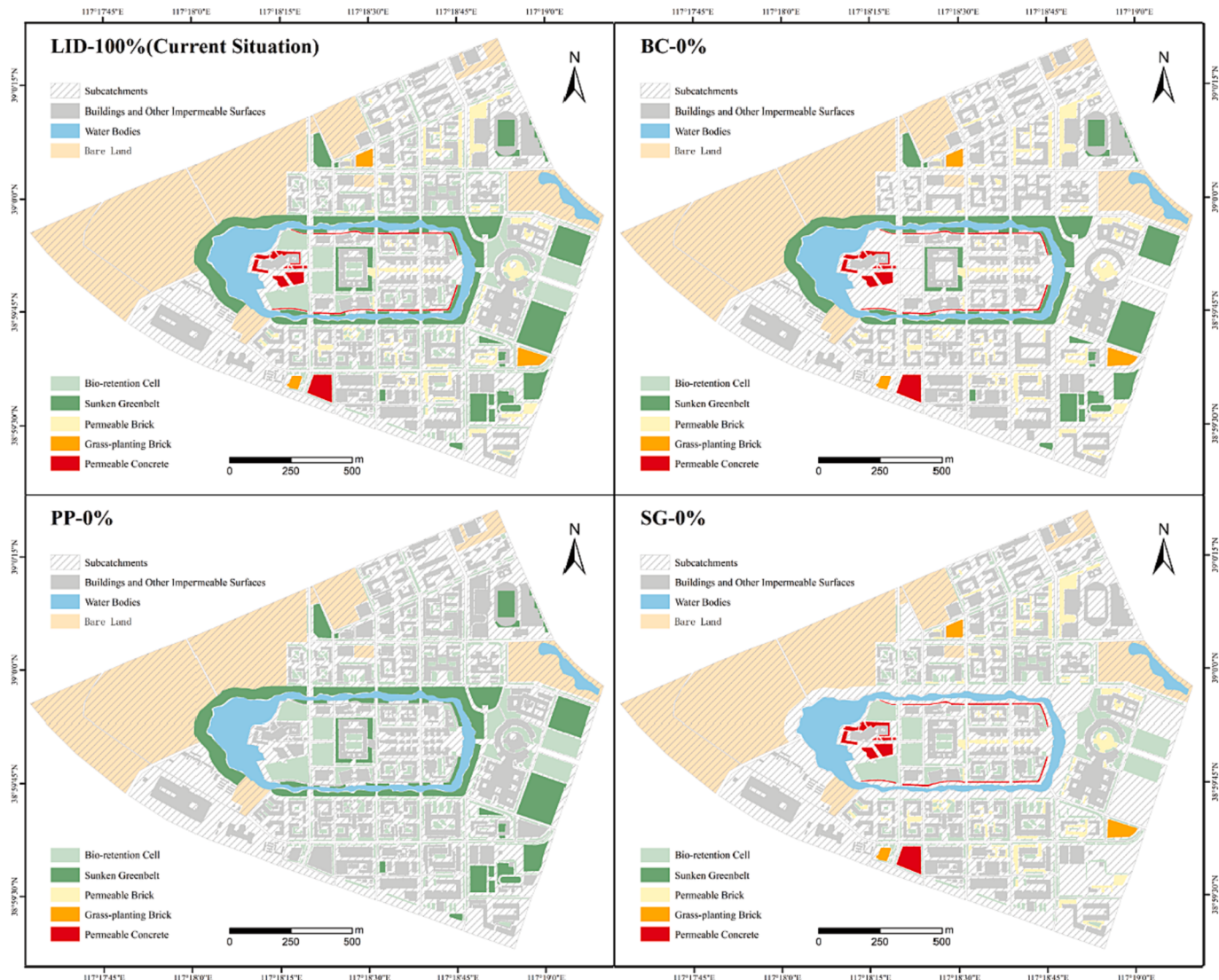


Fig. 5. LID removal scenarios.

3. Results

3.1. Permeable pavement infiltration characteristics and parameter determination

The artificial rainfall system was used to conduct the constant rainfall intensity infiltration experiment for two permeable pavements. The Horton infiltration model has fewer parameters and can describe the variation of infiltration rate with time course, which makes it suitable for application in small urban watersheds. Therefore, the experimental results are fitted with the Horton infiltration model to quantitatively analyze the infiltration characteristics of permeable pavements. The Horton infiltration model (Horton, 1940) describes the infiltration capacity as an exponential relationship with time, which is calculated as follows:

$$f(t) = f_c + (f_0 - f_c)e^{-kt} \quad (6)$$

where $f(t)$ is the infiltration rate, mm/s, f_c is the stable infiltration rate, mm/s, f_0 is the initial infiltration rate, mm/s, k is the empirical coefficient which is constant.

The results of the independent fitting of the permeable pavements under the three experiments are shown in Table S3. The determination coefficient R^2 ranged from 0.63 to 0.93 for the permeable concrete and

from 0.65 to 0.79 for the grass-planting brick, which presented a good fit, and the Horton infiltration model was suitable for both permeable pavements. In order to increase the sample size, the experimental data of each group were fitted in concatenate, and the results of the concatenate fit are shown in Table 2 and Fig. 7. From Table 2, it can be seen that the permeable concrete has a concatenate fitted R^2 of 0.77 and the grass-planting brick of 0.65. The overall trend is shown in Fig. 7, where the permeable concrete exhibits a large initial infiltration rate but a faster decay, and the grass-planting brick has a slower decay in the infiltration process, with a greater stable infiltration rate and infiltration capacity than the permeable concrete. That is caused by the fact that the upper structure of the permeable concrete is a high-permeability macroporous material with a large initial infiltration rate, while the grass-planting brick has a larger initial water storage due to the retention effect of planted grass.

The LID parameters in the SWMM model are divided into two main categories, one for measured parameters such as thickness and area, and the other for calibrated parameters, the most important of which is the infiltration parameter. In common studies, LID infiltration parameters are obtained from Model Manuals, References, or calibrated with subcatchment parameters, all of which have uncertainties compared to the parameters obtained from fundamental LID experiments. Therefore, in this paper, the LID infiltration parameters obtained from the above

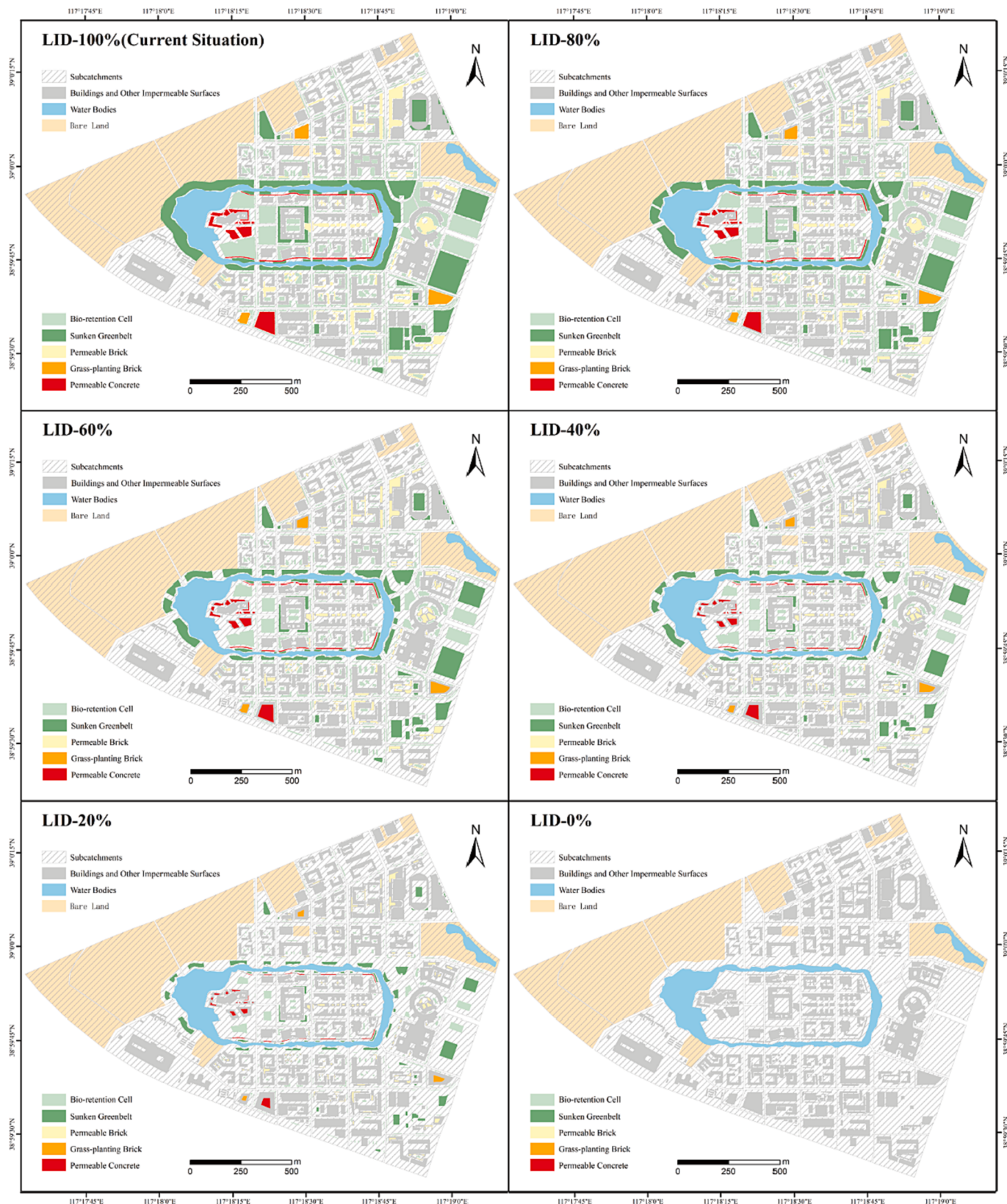


Fig. 6. LID density reduction scenarios.

prototype experiments are integrated into the SWMM model to improve the reliability of the LID parameters. Specifically, the concatenate fitted parameters are used to obtain the mean infiltration rate by using the Equi-area Method, and the results are shown in Fig. 7. After converting

the unit as required in the SWMM model, the mean infiltration rate of permeable concrete and the grass-planting brick were 95 mm/hr and 190 mm/hr, respectively.

Table 2

Results of infiltration experiments on permeable pavements with constant rainfall intensity.

Underlying surfaces type	f_0 (mm/s)	f_c (mm/s)	k	R^2
Permeable concrete	0.3087	0.0159	1.3214	0.77
Grass-planting brick	0.0993	0.0258	0.1189	0.65

3.2. Parameter calibration and model verification

The MIKE21 model in this paper is only used for 2D surface flow simulations, and the effects of wind and Coriolis force are ignored. Thus, the main parameters to be calibrated are the hydrological and hydrodynamic parameters in the SWMM model. The parameters in the SWMM model, such as conduit diameter, length, and junction elevation, were extracted from the drainage system in the study area. Parameters such as subcatchment area, impervious rate, and mean slope were calculated using ArcGIS. The infiltration parameters for permeable concrete and grass-planting brick were obtained from the LID experiments as described in section 3.1. The calibrated parameters in the SWMM model, such as Manning's roughness, depression storage, and subcatchment infiltration parameters, are calibrated via the observed water depths and the MIKE21 simulated water depths in the river.

In this paper, the model parameters were calibrated using the field-observed rainfall and water depth data on 9 October 2017, and the model was verified with the field-observed rainfall and water depth data on 23 July 2018 (Fig. 8). The results of the model parameter are shown in Table S4 and Table S5. The simulated and observed water depth of the two historical rainfalls are shown in Fig. 8.

As shown in Fig. 8, the simulated values are in good agreement with the observed values, while the model accuracy is quantitatively evaluated by R^2 , NSE, and RMSE, shown in Table 3. The model had R^2 greater than 0.94, NSE greater than 0.86, and RMSE of 2.5 cm and 5.6 cm in both the calibration and verification. The closer the R^2 is to 1, the better the correlation is between the simulated and the observed data; the closer the NSE is to 1, the better the agreement is between the simulated and the observed data; and the smaller the RMSE, the smaller the error is between the simulated and the observed data. Overall, R^2 , NSE, and RMSE all indicate an excellent model performance in the calibration and verification (Nash and Sutcliffe, 1970; Moriasi et al., 2007; Muthusamy et al., 2021), this it be used for subsequent numerical simulation studies.

3.3. Urban hydrological effects in LID regions

Based on the SWMM and MIKE21 coupled model constructed for the study area, all LID removal and density reduction scenarios were simulated under design rainstorm events of different return periods. Surface hydrological characteristics such as runoff volume, comprehensive runoff coefficient, surcharge volume, inundation area, and inundation depth were obtained to quantitatively analyze the effects of different LID removal and density reduction schemes on urban surface hydrological processes.

3.3.1. Effects of different LID practices on surface hydrological processes

Based on the simulation results, the runoff volumes, comprehensive runoff coefficients, and surcharge volumes for different LID removal scenarios under each return period were calculated (Table 4). As shown in Table 4, no surcharge occurs during the 1-year return period for any scenario. As rainfall increases, the runoff volume, comprehensive runoff coefficient, and surcharge volume all increase. After the LID practices are removed, the runoff volume, the comprehensive runoff coefficient, and the surcharge volume all increase. Nevertheless, the comprehensive runoff coefficient for the SG-0% scenario is much closer to the LID-100%, which indicates that the effect of the sunken greenbelt on runoff control is minimal.

Taking the 100% LID scenario as a reference, the increase rate in runoff volume, inundation area, and inundation depth after the LID removal was calculated (Fig. 9). As shown in Fig. 9, the increase rate in runoff volume, inundation area and inundation depth decrease with the increase of rainfall for each scenario, which indicates that the control capacity of each LID practice gradually decreases when rainfall increases.

As shown in Fig. 9a, the increase in runoff volume under the 1-year return period is BC-0% > PP-0% > SG-0%, and the increase in runoff volume under the 2-year to 4-year return period is PP-0% > BC-0% > SG-0%. It indicates that the bio-retention cell has the best effect on runoff control during the 1-year return period and more frequent light rainfall. When the return period was greater than 2 years, the permeable pavement performed better in runoff control, but the overall effect was closer to that of the bio-retention cell. The increase rate in runoff volume from the sunken greenbelt removal gradually decreased from 32% to 6%, with limited runoff control.

In order to eliminate the influence of the total LID implemented area,

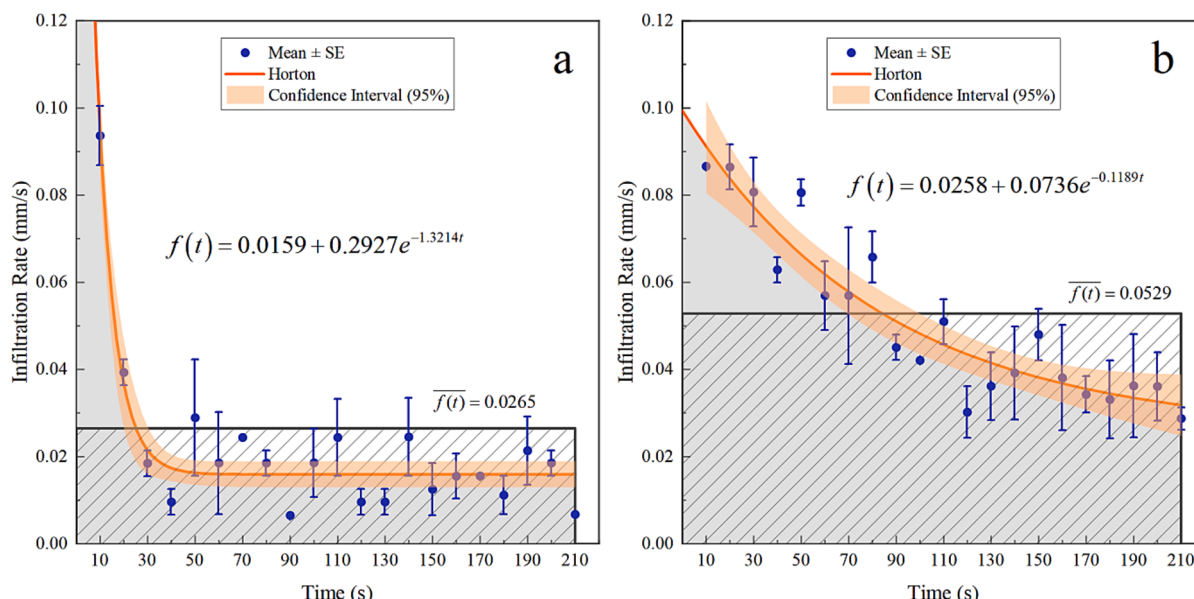


Fig. 7. Results of concatenating fit: (a) permeable concrete; (b) grass-planting brick.

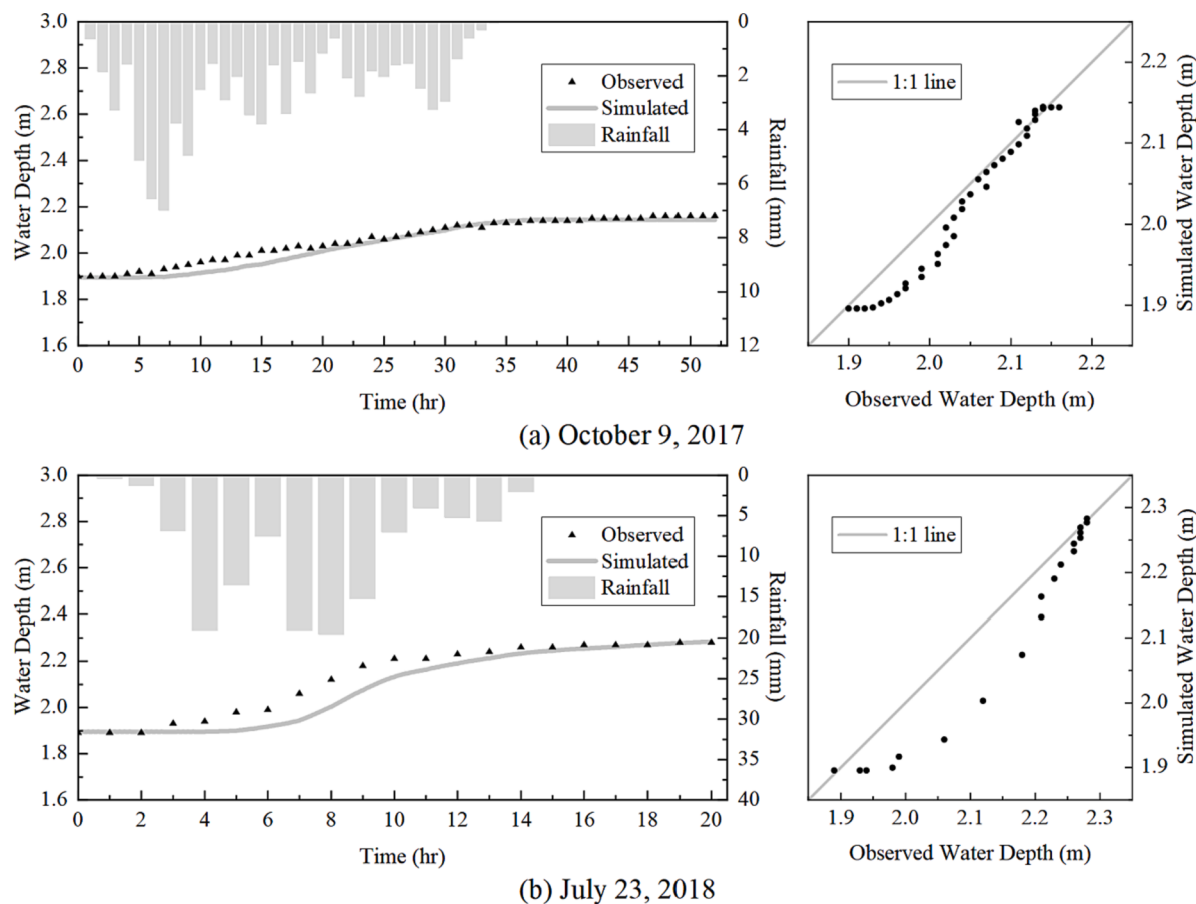


Fig. 8. Observed and simulated water depths of the two historical rainfall events.

Table 3
Model accuracy evaluation results.

Stage	Flooding Data	R ²	NSE	RMSE (cm)
Calibration	20,171,009	0.97	0.92	2.5
Verification	20,180,723	0.94	0.86	5.6

Table 4
Runoff volume, comprehensive runoff coefficient, and surcharge volume under LID removal scenarios.

Scenarios	Characteristics	T = 1	T = 2	T = 3	T = 4
LID-100%	Runoff volume ($\times 10^4$ m ³)	0.23	2.96	3.82	4.47
	Comprehensive runoff coefficient	0.04	0.22	0.25	0.28
BC-0%	Surcharge volume ($\times 10^4$ m ³)	–	0.32	0.86	1.28
	Runoff volume ($\times 10^4$ m ³)	0.42	3.73	4.59	5.23
PP-0%	Comprehensive runoff coefficient	0.07	0.27	0.30	0.32
	Surcharge volume ($\times 10^4$ m ³)	–	0.75	1.27	1.67
SG-0%	Runoff volume ($\times 10^4$ m ³)	0.38	3.80	4.74	5.44
	Comprehensive runoff coefficient	0.07	0.28	0.31	0.34
	Surcharge volume ($\times 10^4$ m ³)	–	0.82	1.42	1.86
	Runoff volume ($\times 10^4$ m ³)	0.30	3.31	4.13	4.74
	Comprehensive runoff coefficient	0.04	0.24	0.27	0.29
	Surcharge volume ($\times 10^4$ m ³)	–	0.54	1.04	1.42

the increased runoff volume from a unit area of each LID practice was calculated (Fig. 9b). As shown in Fig. 9b, for increased runoff volume per unit area, it is always PP-0% > BC-0% > SG-0%, which indicates that

permeable pavement per unit area is the most effective in runoff control. As rainfall increases, permeable pavement per unit area is more effective in runoff control, more than 2 times of bio-retention cell and sunken greenbelt per unit area when the return period reaches 2 years.

As shown in Fig. 9c, in terms of the effect of the inundation area control, it is always PP-0% > BC-0% > SG-0%. The inundation area increases after removing each type of LID practice, but the simulation results show that the inundation region does not change significantly between scenarios for different return periods. Fig. S4 shows the inundation region for each LID removal scenario for the 4-year return period. The distribution characteristics are that no inundation occurs in the central island catchment zone (Fig. 4) where LID practices are concentrated under any of the scenarios. The inundation occurs mainly in the midland catchment zone in the northeast, and maximum inundation depth occurs in the low-lying wetlands in the west.

As shown in Fig. 9d, the increase rate in inundation depth for the PP-0% and BC-0% scenarios are very close under the 2- and 3-year return periods. Under the PP-0% scenario, a slight increase was found for the 4-year return period, and the BC-0% scenario had a decreasing trend, which indicates that both permeable pavement and bio-retention cell perform better in inundation depth control, but the permeable pavement has a more stable control effect. The SG-0% scenario shows an overall decreasing trend, and the control effect is less than 20% under the 4-year return period.

The maximum inundation depth considers the most unfavorable situation and is often used as an important basis for assessing urban flooding losses (Velasco et al., 2016). A boxplot of the maximum inundation depth in the study area for each scenario is shown in Fig. 10. As shown in Fig. 10, 95% of the maximum inundation depths were within 25cm for each scenario. The 25%-75% interval and mean values, show

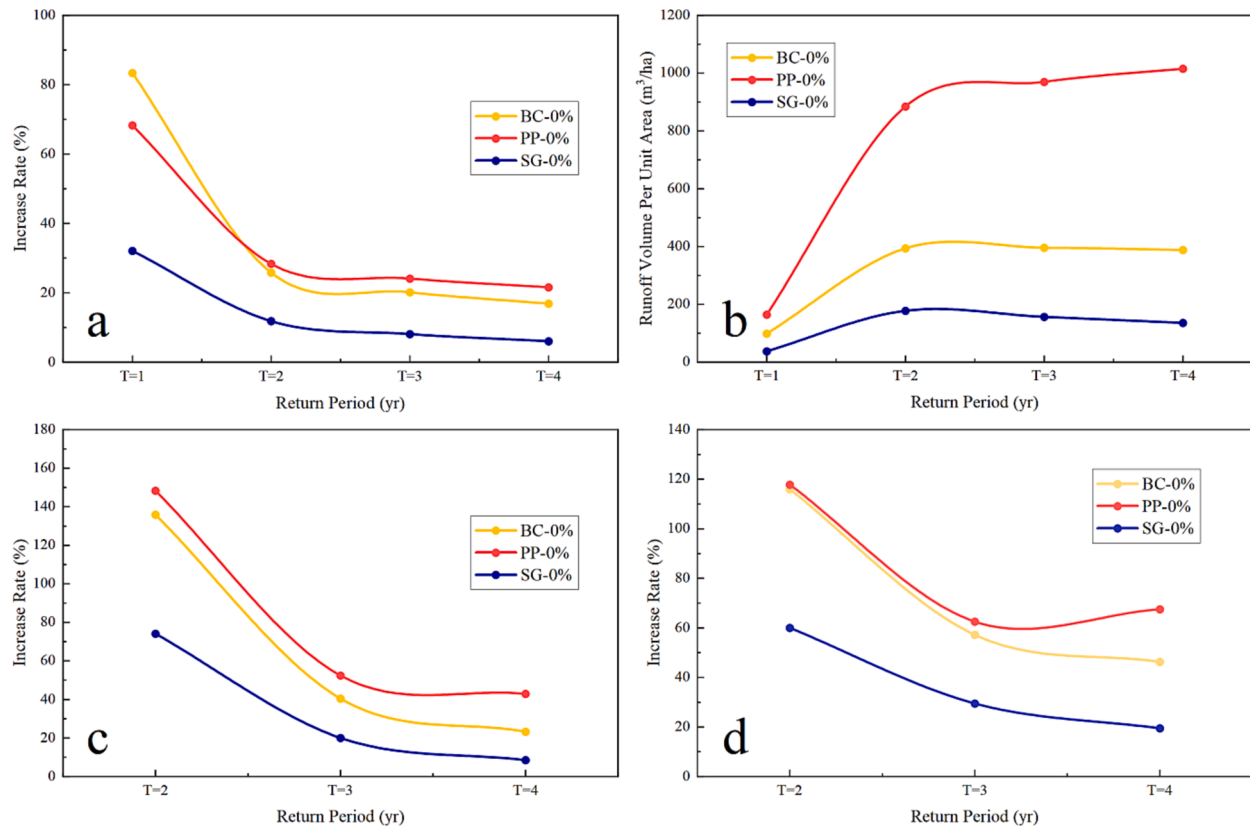


Fig. 9. Trends under different LID removal scenarios: (a) runoff volume; (b) runoff volume per unit area; (c) inundation area; (d) inundation depth.

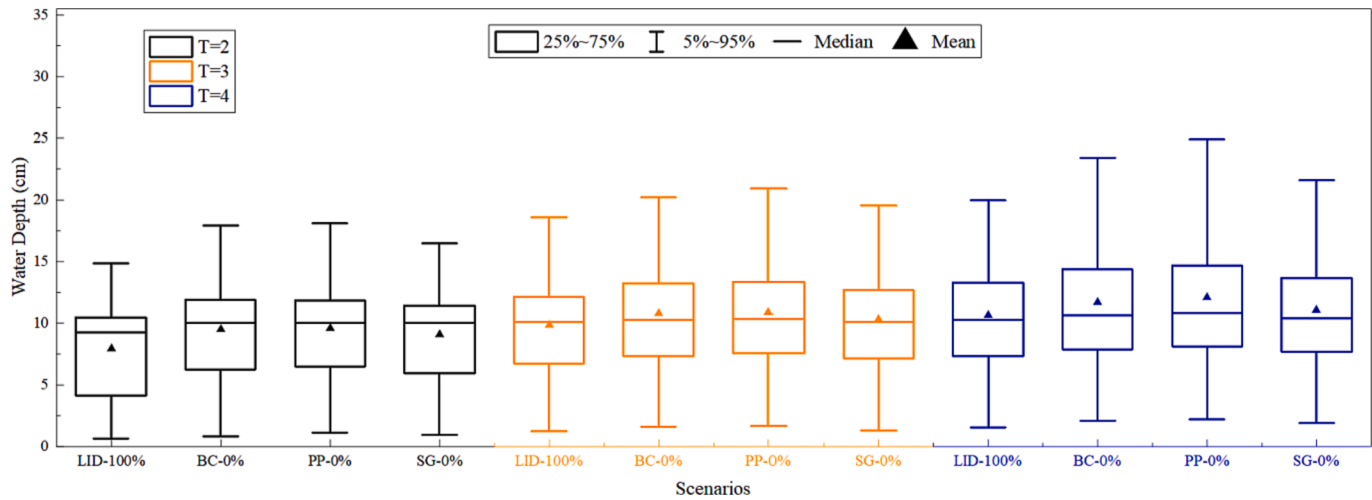


Fig. 10. Maximum inundation depth under LID removal scenarios.

that the maximum inundation depth increased after removing each type of LID practice. The increase was comparatively stable but the 2-year return period shows a more concentrated tendency.

3.3.2. Effects of LID density on surface hydrological processes

Based on the simulation results, the runoff volume, comprehensive runoff coefficient, and surcharge volume were calculated for each LID density reduction scenario under different return periods (Table 5). As shown in Table 5, no surcharge was generated for each LID density reduction scenario under the 1-year return period. The runoff volume, comprehensive runoff coefficient, and surcharge volume all increase with increasing rainfall and decreasing LID density. Under the 1-year

return period, the comprehensive runoff coefficient increases faster after reducing the LID density, which indicates that the 1-year return period and more frequent light rainfall are more sensitive to the LID density.

Taking the LID-100% scenario as a reference, the increase rate in runoff volume, inundation area, and inundation depth after the density reduction of the LID practice was calculated (Fig. 11). As shown in Fig. 11, the increase rate in runoff volume, inundation area and inundation depth all decrease with increasing rainfall and increase with decreasing LID density.

As shown in Fig. 11a, the increase of runoff volume is small for all LID-80% scenarios, and even under the 1-year return period, the

Table 5

Runoff volume, comprehensive runoff coefficient, and surcharge volume under LID density reduction scenarios.

Scenarios	Characteristics	T = 1	T = 2	T = 3	T = 4
LID-100%	Runoff volume ($\times 10^4 \text{ m}^3$)	0.23	2.96	3.82	4.47
	Comprehensive runoff coefficient	0.04	0.22	0.25	0.28
LID-80%	Surcharge volume ($\times 10^4 \text{ m}^3$)	–	0.32	0.86	1.28
	Runoff volume ($\times 10^4 \text{ m}^3$)	0.27	3.31	4.19	4.85
LID-60%	Comprehensive runoff coefficient	0.05	0.24	0.28	0.30
	Surcharge volume ($\times 10^4 \text{ m}^3$)	–	0.55	1.09	1.50
LID-40%	Runoff volume ($\times 10^4 \text{ m}^3$)	0.35	3.73	4.62	5.28
	Comprehensive runoff coefficient	0.06	0.27	0.31	0.33
LID-20%	Surcharge volume ($\times 10^4 \text{ m}^3$)	–	0.79	1.34	1.75
	Runoff volume ($\times 10^4 \text{ m}^3$)	0.51	4.21	5.09	5.74
LID-0%	Comprehensive runoff coefficient	0.09	0.31	0.34	0.35
	Surcharge volume ($\times 10^4 \text{ m}^3$)	–	1.05	1.59	1.99
LID-0%	Runoff volume ($\times 10^4 \text{ m}^3$)	0.86	4.74	5.60	6.23
	Comprehensive runoff coefficient	0.15	0.35	0.37	0.38
LID-0%	Surcharge volume ($\times 10^4 \text{ m}^3$)	–	1.34	1.86	2.26
	Runoff volume ($\times 10^4 \text{ m}^3$)	1.49	5.33	6.17	6.78
LID-0%	Comprehensive runoff coefficient	0.26	0.39	0.41	0.42
	Surcharge volume ($\times 10^4 \text{ m}^3$)	–	1.64	2.15	2.54

increase rate of runoff volume is less than 20%, which indicates that the small reduction in density of the LID practice has a small impact on runoff volume. The most significant increases in runoff volume occurred in the LID-0% scenario, particularly under the 1-year return period,

where the increase was quite significant, with a dramatic increase from 278% to 551%. Which suggests that even a tiny percentage (4% of the watershed area) of LID practices implemented can be effective in runoff control, and the study by Ghodsi et al. (2020) proposed similar conclusions.

As shown in Fig. 11b, the increase in inundation area after LID density reduction has a relatively stable increasing trend. Compared to the effect on runoff volume, even a 20% reduction in LID density significantly affects the inundation area under the 1-year return period. Based on the simulation results, the inundation region is generally consistent across the LID density reduction scenarios. Fig. S5 shows the inundation region for the LID density scenario under the 4-year return period, and the overall distribution characteristics are similar to the LID removal scenario. Noteworthy, the central island catchment zone does not inundate even under the LID-0% scenario.

As shown in Fig. 11c, the increase in inundation depth for the LID-80% and LID-60% scenarios is very close under the 3- and 4-year return periods. It indicates that the reduction of the LID density by 20–40% has minimal effect on the inundation depth after the return period reaches 3 years. Meanwhile, large increase in inundation depth under the 2-year to 4-year return period occurred in the LID-20%, LID-40%, and LID-60% scenarios, respectively. This indicates that the effect of LID density on inundation depth is strongly related to rainfall.

The maximum inundation depths under the LID density reduction scenarios are shown in Fig. 12. The 95% quantile inundation depths grow faster after the density reduction, while the 25%-75% interval and 5% quantile inundation depths grow slowly. It indicates that the reduction in LID density has a greater impact on regions with deeper ponding. Similarly, the 25%-75% interval under the 2-year return period is significantly reduced and shifted upwards by reducing the density of

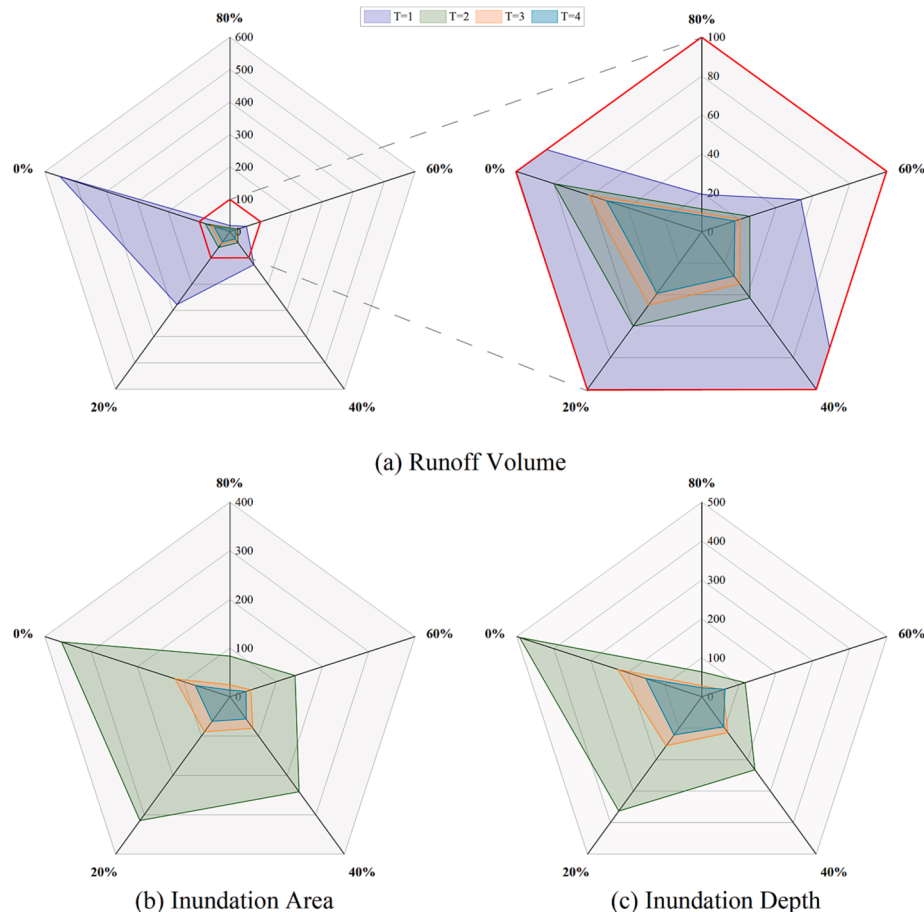


Fig. 11. Increase rate after LID density reduction: (a) runoff volume; (b) inundation area; (c) inundation depth.

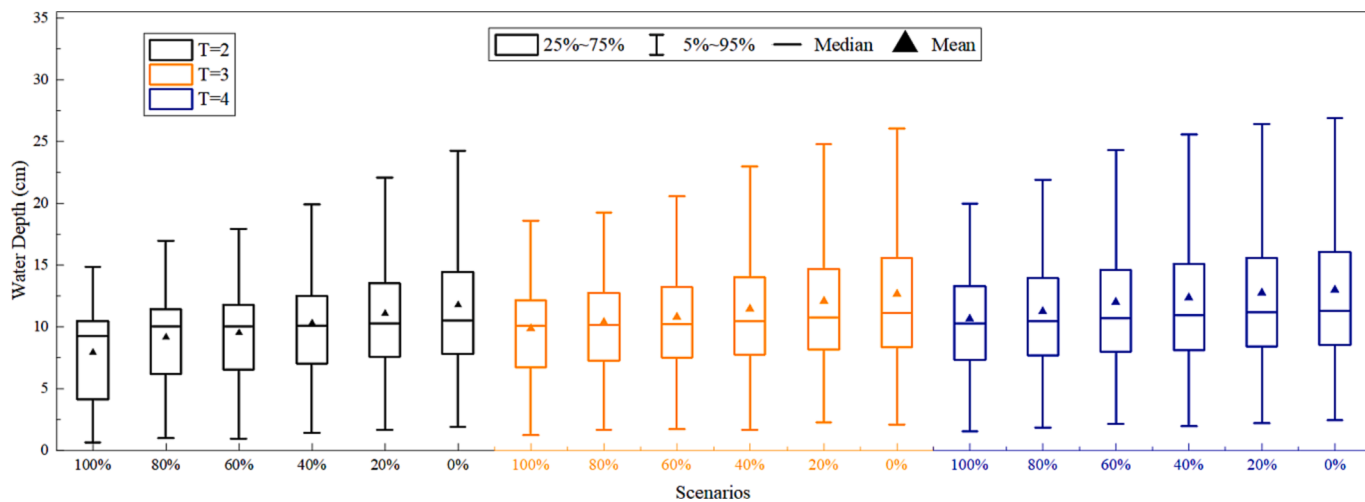


Fig. 12. Maximum inundation depth under LID density reduction scenarios.

LID. This suggests that LID density reduction has a greater impact on the maximum inundation depth at a light rainfall.

Both the LID removal scenarios and density reduction scenarios show a significant increase rate in runoff volume under the 1-year return period and a rapid decay in increase rate after reaching the 2-year return period. This suggests that the LID practice has the best runoff control effect during the 1-year return period and more frequent light rainfall, and our work confirms this understanding from the perspective in LID regions.

The study by Zhao et al. (2021) on flood losses suggests the greater possibility of flood losses due to inundation depth with increasing rainfall. Comparing the relationship between the mean and median of maximum inundation depth, it is found that the proportion of maximum inundation depth above the mean increases after either LID removal or density reduction. Considering the strong relationship between maximum inundation depth and flood risk, it can be considered that LID removal and density reduction lead to a similar effect, which is the increased possibility of flood risk due to increasing inundation depth.

4. Discussion

The infiltration performance of permeable pavement significantly influences its low impact development function (Song et al., 2021). Taking advantage of the clear and controllable indoor experimental conditions (Sambito et al., 2021), analyzing its infiltration characteristics through prototype experiments is necessary and key to improving the accuracy of LID parameters in the numerical model.

In order to ensure the rationality and reliability of the combination of physical experiments and numerical simulations, we have made great efforts, such as scaling the prototype permeable pavement according to the design drawings and instructions for the experiments. Considering the significant influence of the antecedent dry period in daytime (ADP daytime) on the infiltration performance (Wu et al., 2022), setting the same ADP daytime in the SWMM model as in the experiments. Using the Equi-area Method which is commonly used in hydrological data processing to generalize the mean infiltration rate of the permeable pavement. However, due to the difference in age and maintenance conditions between the field permeable pavement in the study area and the experimental permeable pavement (Kumar et al., 2016; Sambito et al., 2021), the uncertainty was inevitably introduced into the numerical model.

With the development of data collection techniques and urban hydrological models, the use of numerical simulations to study the urban hydrological effects is an inevitable development trend (Xu et al., 2020). Determining the LID infiltration parameters through physical

experiments to improve the reliability of numerical simulations is also an inevitable requirement for the development of refined simulations. In general, our efforts have provided a set of reliable methods to improve the accuracy of LID parameters in urban hydrological models, which is of great significance for reference.

The maximum increase rate in runoff coefficient after different LID practice removal is only 21%, that is due to 60–80% of the LID is still remained in the study area. Consistent with the conclusion that reducing a small percentage of LID density has little effect on runoff proposed in Section 3.2. Meanwhile, even under the 4-year return period LID-0% scenario, the comprehensive runoff coefficient is only 0.42. That is due to the high percentage of permeable area in the study area. The mean permeable area proportion is still as high as 65% under the no LID practice scenario, thus checking the empirical values of the urban comprehensive runoff coefficient in the *China Drainage Manual* (1990), 0.42 is within the empirical value range.

With the limitations of the experimental conditions, this study only selects permeable concrete and grass-planting brick for physical experiments, and permeable brick and other LID infiltration parameters are obtained by calibrating observed water depth data. In future studies, the LID infiltration experiments can be completed further to explore the local hydrological effect of LID practice. Furthermore, based on the coupled model constructed in this paper, combined with the theory of flood risk, the effect of LID removal or density reduction on flood risk under extreme precipitation conditions can be further discussed.

5. Conclusions

This paper quantitatively analyses the infiltration characteristics of typical permeable pavements through prototype permeable pavement infiltration experiments. On this basis, the measured infiltration parameters are adopted in a 1D-2D coupled urban hydrological model constructed for the study area. Then the effects of LID removal and density reduction on surface hydrological processes in LID regions are further explored. The main conclusions are as follows:

- (1) The infiltration process of both permeable pavements can be described by the Horton infiltration model, with R^2 ranging from 0.63 to 0.93. The infiltration process of permeable concrete exhibits a large initial infiltration rate but decays rapidly, while the infiltration process of grass-planting brick decays relatively slowly. The stable infiltration rate and infiltration capacity the latter are higher than those of permeable concrete. The mean infiltration rates measured for permeable concrete and grass-planting brick were 95 mm/hr and 190 mm/hr, respectively.

- (2) The bio-retention cell was most effective in runoff control during frequent light rainfall, while permeable pavement performed better with increasing rainfall. Permeable pavement per unit area has the best runoff control, especially after the return period reaches 2 years. Permeable pavement performs best in terms of inundation area and inundation depth control. Bio-retention cell is also effective for inundation depth control, but permeable pavement performs much stably. Sunken greenbelt has limited effectiveness in terms of runoff volume, inundation area, and depth control.
- (3) With the 1-year return period and more frequent light rainfall, a 20% reduction of LID density has a small impact on runoff but a significant impact on the inundation area. Meanwhile, the implementation of even a tiny percentage (4% of the catchment area) of LID practice is effective in runoff control. The effect of LID density on inundation depth is much related to rainfall. A 20%-40% reduction in LID density has minimal effect on inundation depth after the return period reaches 3 years.
- (4) The LID removal and density reduction scenarios show that the effectiveness of LID control decreased with increasing rainfall, with the best control effectiveness under the 1-year return period. Meanwhile, LID removal or density reduction has little effect on the inundation region but will lead to an increased possibility of flood risk due to increasing inundation depth.

CRediT authorship contribution statement

Lidong Zhao: Conceptualization, Methodology, Investigation, Software, Formal analysis, Visualization, Writing – original draft. **Ting Zhang:** Validation, Formal analysis, Writing – review & editing. **Jianzhu Li:** Validation, Writing – review & editing. **Libin Zhang:** Investigation. **Ping Feng:** Supervision, Funding acquisition.

Declaration of Competing Interest

The authors declare that they have no known competing financial interests or personal relationships that could have appeared to influence the work reported in this paper.

Data availability

The authors do not have permission to share data.

Acknowledgments

Thanks to Jiaxin Zhang and Ziqi Wang from Tianjin University for their assistance in the field experiment. Thanks to the Department of Logistics and Infrastructure of Tianjin University for providing the primary modeling data. Thanks to Associate Professor Liang Chen from Tianjin University for providing the observed data on rainfall and water depth.

Funding

This work was supported by the National Natural Science Foundation of China (51779165), Natural Science Foundation of Tianjin (20JCQNJC01960), National Key Research and Development Program of China (2021YFD1700400) and Yunnan Fundamental Research Projects (202201AU070001).

Appendix A. Supplementary data

Supplementary data to this article can be found online at <https://doi.org/10.1016/j.jhydrol.2023.129191>.

References

- Ahiablame, L.M., Engel, B.A., Chaubey, I., 2012. Effectiveness of Low Impact Development Practices: Literature Review and Suggestions for Future Research. *Water Air Soil Pollut.* 223 (7), 4253–4273. <https://doi.org/10.1007/s11270-012-1189-2>.
- Baek, S., Choi, D., Jung, J., Lee, H.J., Lee, H., Yoon, K., Cho, K.H., 2015. Optimizing Low Impact Development (LID) for Stormwater Runoff Treatment in Urban Area, Korea: Experimental and Modeling Approach. *Water Res.* 86, 122–131. <https://doi.org/10.1016/j.watres.2015.08.038>.
- Che, W., Zhao, Y., Li, J., Wang, W., Wang, J., Wang, S., Gong, Y., 2015. Explanation of Sponge City Development Technical Guide: Basic Concepts and Comprehensive Goals. *China Water & Wastewater.* 31 (8), 1–5. <https://doi.org/10.19853/j.zgjwps.1000-4602.2015.08.001>.
- M. Dilley R.S. Chen U. Deichmann A.L. Lerner Lam M. Arnold Natural Disaster Hotspots: A Global Risk Analysis 2005 Washington D.C.
- DHI, 2022. MIKE21 Flow Model: Scientific Documentation. accessed on 31 October 2022. https://manuals.mikepoweredbydhi.help/latest/Coast_and_Sea/M21HDFST_Scientific_Doc.pdf.
- Eckart, K., McPhee, Z., Bolisetti, T., 2018. Multiobjective Optimization of Low Impact Development Stormwater Controls. *J. Hydrol.* 562, 564–576. <https://doi.org/10.1016/j.jhydrol.2018.04.068>.
- H. Fisher B. Burkhardt A. Brebner LID on the Sc Coastal Plain: Benefits Costs, and Constraints, Second National Low Impact Development Conference 2007 Wilmington, United States.
- Ghodsi, S.H., Zahmatkesh, Z., Goharian, E., Kerachian, R., Zhu, Z., 2020. Optimal Design of Low Impact Development Practices in Response to Climate Change. *J. Hydrol.* 580, 124266 <https://doi.org/10.1016/j.jhydrol.2019.124266>.
- Gilroy, K.L., McCuen, R.H., 2009. Spatio-Temporal Effects of Low Impact Development Practices. *J. Hydrol.* 367 (3–4), 228–236. <https://doi.org/10.1016/j.jhydrol.2009.01.008>.
- Hamel, P., Daly, E., Fletcher, T.D., 2013. Source-Control Stormwater Management for Mitigating the Impacts of Urbanisation on Baseflow: A review. *J. Hydrol.* 485, 201–211. <https://doi.org/10.1016/j.jhydrol.2013.01.001>.
- Han, R., Li, J., Li, Y., Xia, J., Gao, X., 2021. Comprehensive Benefits of Different Application Scales of Sponge Facilities in Urban Built Areas of Northwest China. *Ecohydrolog. Hydrobiol.* 21 (3), 516–528. <https://doi.org/10.1016/j.ecohyd.2021.08.008>.
- Horton, R.E., 1940. An Approach Toward a Physical Interpretation of Infiltration-Capacity. *Soil Sci. soc. proceedings.* 5 (C), 399–417. <https://doi.org/10.2136/sssaj1941.036159950005000C0075x>.
- Hou, J., Zhang, Y., Tong, Y., Guo, K., Qi, W., Hinkelmann, R., 2019. Experimental Study for Effects of Terrain Features and Rainfall Intensity on Infiltration Rate of Modelled Permeable Pavement. *J. Environ. Manage.* 243, 177–186. <https://doi.org/10.1016/j.jenvman.2019.04.096>.
- Huang, G., 2018. Discrimination of Relationship Between Urban Storm Waterlogging Prevention and Sponge City Construction. *China Flood & Drought Management.* 28, 8–14. <https://doi.org/10.16867/j.cnki.cfdm.20180112.001>.
- IPCC 2021: Summary for Policymakers. In: Climate Change 2021: The Physical Science Basis. <https://www.ipcc.ch/report/ar6/wg1/#FullReport> (accessed on 31 October 2022).
- Jia, S., 2017. China Should Prioritize Waterlogging Prevention for Recent Urban Storm Water Management. *Water Resources Protection.* 32 (2), 13–15. <https://doi.org/10.3880/j.issn.1004-6933.2017.02.003>.
- Jia, H., Wang, Z., Zhen, X., Clar, M., Yu, S.L., 2017. China's Sponge City Construction: A Discussion on Technical Approaches. *Front. Env. Sci. Eng.* 11 (4), 18. <https://doi.org/10.1007/s11783-017-0984-9>.
- Kamali, M., Delkash, M., Tajrishy, M., 2017. Evaluation of Permeable Pavement Responses to Urban Surface Runoff. *J. Environ. Manage.* 187, 43–53. <https://doi.org/10.1016/j.jenvman.2016.11.027>.
- Kumar, K., Kozak, J., Hundal, L., Cox, A., Zhang, H., Granato, T., 2016. In-Situ Infiltration Performance of Different Permeable Pavements in a Employee Used Parking Lot - A Four-Year Study. *J. Environ. Manage.* 167, 8–14.
- Li, F., Liu, Y., Engel, B.A., Chen, J., Sun, H., 2019. Green Infrastructure Practices Simulation of the Impacts of Land Use on Surface Runoff: Case study in Ecorse River Watershed. Michigan. *J. Environ. Manage.* 233, 603–611. <https://doi.org/10.1016/j.jenvman.2018.12.078>.
- Lisenbee, W.A., Hathaway, J.M., Winston, R.J., 2022. Modeling Bioretention Hydrology: Quantifying the Performance of DRAINMOD-Urban and the SWMM LID Module. *J. Hydrol.* 612, 128179 <https://doi.org/10.1016/j.jhydrol.2022.128179>.
- Liu, Y., Ahiablame, L.M., Bralts, V.F., Engel, B.A., 2015. Enhancing a Rainfall-Runoff Model to Assess the Impacts of BMPs and LID Practices on Storm Runoff. *J. Environ. Manage.* 147, 12–23. <https://doi.org/10.1016/j.jenvman.2014.09.005>.
- Miu, R., 2007. *Principles of Hydrology*, 1st ed. Beijing, China.
- Moriasi, D.N., Arnold, J.G., Van Liew, M.W., Bingner, R.L., Harmel, R.D., Veith, T.L., 2007. Model Evaluation Guidelines for Systematic Quantification of Accuracy in Watershed Simulations. *Trans. ASABE* 50, 885–900. <https://citeserx.ist.psu.edu/viewdoc/download?doi=10.1.1.532.2506&rep=rep1&type=pdf>.
- Muthusamy, M., Casado, M.R., Butler, D., Leinster, P., 2021. Understanding the Effects of Digital Elevation Model Resolution in Urban Fluvial Flood Modelling. *J. Hydrol.* 596, 126088 <https://doi.org/10.1016/j.jhydrol.2021.126088>.
- Nash, J.E., Sutcliffe, J.V., 1970. River Flow Forecasting Through Conceptual Models Part I-A Discussion of Principles. *J. Hydrol.* 10, 282–290. [https://doi.org/10.1016/0022-1694\(70\)90255-6](https://doi.org/10.1016/0022-1694(70)90255-6).

- Peng, Y., Li, Z., Ding, Y., 2020. Research on the Schemes Formulation and Optimization Method of Sponge Reconstruction in a Highway Service Area. *Water Sci. Technol.* 82 (12), 2889–2901. <https://doi.org/10.2166/wst.2020.539>.
- Qiu, J., 2012. Urbanization Contributed to Beijing Storms. *Nature*. <https://doi.org/10.1038/nature.2012.11086>.
- Rossman, L.A., 2015. Storm Water Management Model User's Manual Version 5.1. https://www.epa.gov/sites/default/files/2019-02/documents/epaswmm5_1_manual_master_8-2-15.pdf (accessed on 31 October 2022).
- Rui, X., Jiang, C., Chen, Q., Ding, X., 2015. Principle Analysis and Application of Storm Water Management Model on Stimulating Rainfall-Runoff. *Adv. Sci. Technol. Water Resour.* 35 (4), 1–5. <https://doi.org/10.3880/j.issn.1006-7647.2015.04.001>.
- Sambito, M., Severino, A., Freni, G., Neduzha, L., 2021. A Systematic Review of The Hydrological, Environmental and Durability Performance of Permeable Pavement Systems. *Sustainability-Basel.* 13 (8), 4509. <https://doi.org/10.3390/su13084509>.
- Sanudo, E., Cea, L., Puertas, J., 2020. Modelling Pluvial Flooding in Urban Areas Coupling the Models Iber and SWMM. *Water*. 12 (9), 2647. <https://doi.org/10.3390/w12092647>.
- Shafique, M., Kim, R., 2015. Low impact Development Practices: A Review of Current Research and Recommendations for Future Directions. *Ecol. Chem. Eng. S* 22 (4), 543–563. <https://doi.org/10.1515/ecces-2015-0032>.
- Son, C., Hyun, K., Kim, D., Baek, J., Ban, Y., 2017. Development and Application of a Low impact Development (LID)-Based District Unit Planning Model. *Sustainability-Basel.* 9 (1), 145. <https://doi.org/10.3390/su9010145>.
- Song, J., Wang, J., Wang, W., Peng, L., Li, H., Zhang, C., Fang, X., 2021. Comparison Between Different Infiltration Models to Describe the Infiltration of Permeable Brick Pavement System Via a Laboratory-Scale Experiment. *Water Sci. Technol.* 84 (9), 2214–2227. <https://doi.org/10.2166/wst.2021.437>.
- Sun, Y., Wei, X., Pomeroy, C.A., 2011. Review of Current Research and Future Directions of Low impact Development Practices for Storm Water. *Adv. Water Sci.* 22 (2), 287–293. <https://doi.org/10.14042/j.cnki.32.1309.2011.02.008>.
- Tianjin Housing and Urban-Rural Construction Commission, 2016. The Tianjin Sponge City Construction Technical Guidelines. accessed on 31 October 2022. https://zfcxjs.tj.gov.cn/ztl_70/bzgf/xxbz/xxbzgf/202010/t20201029_4031124.html.
- Tsihrintzis, V.A., Sidan, C.B., 2008. ILLUDAS and PSRM-QUAL Predictive Ability in Small Urban Areas and Comparison with Other Models. *Hydrol. Process.* 22 (17), 3321–3336. <https://doi.org/10.1002/hyp.6914>.
- Velasco, M., Cabello, À., Russo, B., 2016. Flood Damage Assessment in Urban Areas. Application to the Raval District of Barcelona Using Synthetic Depth Damage Curves. *Urban Water J.* 13 (4), 426–440. <https://doi.org/10.1080/1573062X.2014.994005>.
- Wu, Y., Li, J., Lin, C., Guo, X., Zhang, X., 2022. Field Test of Bottom Outflow Control Efficiency in Permeable Pavement with Underdrainage. *China Water Wastewater.* 38 (11), 126–132. <https://doi.org/10.19853/j.zgjzsps.1000-4602.2022.11.022>.
- Wu, Z., Zhou, Y., Wang, H., Jiang, Z., 2020. Depth Prediction of Urban Flood under Different Rainfall Return Periods Based on Deep Learning and Data Warehouse. *Sci. Total Environ.* 716, 137077. <https://doi.org/10.1016/j.scitotenv.2020.137077>.
- Xu, Z., Chen, H., Ren, M., Chen, T., 2020. Progress on Disaster Mechanism and Risk Assessment of Urban Flood/Waterlogging Disasters in China. *Adv. Water Sci.* 31 (5), 713–724. <https://doi.org/10.14042/j.cnki.32.1309.2020.05.008>.
- Xu, T., Engel, B.A., Shi, X., Leng, L., Jia, H., Yu, S., Liu, Y., 2018. Marginal-Cost-Based Greedy Strategy (MCGS): Fast and Reliable Optimization of Low impact Development (LID) Layout. *Sci. Total Environ.* 640–641, 570–580. <https://doi.org/10.1016/j.scitotenv.2018.05.358>.
- Yang, L., Li, J., Kang, A., Li, S., Feng, P., 2020. The Effect of Nonstationarity in Rainfall on Urban Flooding Based on Coupling SWMM and MIKE21. *Water Resour. Manag.* 34 (4), 1535–1551. <https://doi.org/10.1007/s11269-020-02522-7>.
- Yang, W., Zhang, J., Krebs, P., 2022. Low impact Development Practices Mitigate Urban Flooding and Non-Point Pollution under Climate Change. *J. Clean. Prod.* 347, 131320. <https://doi.org/10.1016/j.jclepro.2022.131320>.
- Ye, C., Xu, Z., 2022. Simulation of Fluvial/Pluvial Flooding Processes in a Typical Area Considering Role of Low impact Development (LID) Measures and Joint Operation for Hydraulic Structures: Case Study in Fuzhou City. *J. Hydraul. Eng.* 53 (7), 833–844. <https://doi.org/10.13243/j.cnki.slxh.20220220>.
- Yin, D., Chen, Z., Li, Q., Jia, H., Liu, Z., Shen, L., Ahmad, S., 2021. Influence of Rainfall Characteristics on Runoff Control of a Sponge Reconstructed Community in a Rainy City. *J. Tsinghua Univ. (Sci. & Technol.)* 61 (1), 50–56. <https://doi.org/10.16511/j.cnki.qhdxxb.2020.25.029>.
- Zhang, Z., Chang, J., 1990. *Drainage Design Manual*, 1st ed. Beijing, China.
- Zhang, H., Cheng, X., Zhao, D., Hairong, M., 2018. Analyzing the Contribution of High Resolution Water Range in Dividing Catchment Based on D8 Algorithm. https://www.researchgate.net/publication/328985516_Analyzing_the_Contribution_of_High_Resolution_Water_Range_in_Dividing_Catchment_Based_on_D8_Algorithm. (accessed on 31 October 2022).
- Zhang, J., Song, M., Wang, G., He, R., Wang, X., 2014b. Development and Challenges of Urban Hydrology in A Changing Environment: I: Hydrological Response to Urbanization. *Adv. Water Sci.* 25 (4), 594–605. <https://doi.org/10.14042/j.cnki.32.1309.2014.04.020>.
- Zhang, D., Yan, D., Wang, Y., Lu, F., Liu, S., 2014a. Research Progress on Risk Assessment and Integrated Strategies for Urban Pluvial Flooding. *Journal of Catastrophology.* 29 (1), 144–149. <https://doi.org/10.3969/j.issn.1000-811X.2014.01.026>.
- Zhao, L., Zhang, T., Fu, J., Li, J., Cao, Z., Feng, P., 2021. Risk Assessment of Urban Floods Based on a SWMM-MIKE21-Coupled Model Using GF-2 Data. *Remote Sens-Basel.* 13 (21), 4381.